

Mechanical Properties of a Series of Macro- and Nano-Dimensional Organic Cocrystals Correlate with Atomic Polarizability

Thilini P. Rupasinghe, Kristin M. Hutchins, Bimali S Bandaranayake, Suman Ghorai, Chandana Karunatilake, Dejan-Krešimir Bušar, Dale C. Swenson, Mark A Arnold, Leonard R. MacGillivray, and Alexei V Tivanski

J. Am. Chem. Soc., **Just Accepted Manuscript** • DOI: 10.1021/jacs.5b07873 • Publication Date (Web): 25 Sep 2015

Downloaded from <http://pubs.acs.org> on September 25, 2015

Just Accepted

“Just Accepted” manuscripts have been peer-reviewed and accepted for publication. They are posted online prior to technical editing, formatting for publication and author proofing. The American Chemical Society provides “Just Accepted” as a free service to the research community to expedite the dissemination of scientific material as soon as possible after acceptance. “Just Accepted” manuscripts appear in full in PDF format accompanied by an HTML abstract. “Just Accepted” manuscripts have been fully peer reviewed, but should not be considered the official version of record. They are accessible to all readers and citable by the Digital Object Identifier (DOI®). “Just Accepted” is an optional service offered to authors. Therefore, the “Just Accepted” Web site may not include all articles that will be published in the journal. After a manuscript is technically edited and formatted, it will be removed from the “Just Accepted” Web site and published as an ASAP article. Note that technical editing may introduce minor changes to the manuscript text and/or graphics which could affect content, and all legal disclaimers and ethical guidelines that apply to the journal pertain. ACS cannot be held responsible for errors or consequences arising from the use of information contained in these “Just Accepted” manuscripts.

Mechanical Properties of a Series of Macro- and Nano-Dimensional Organic Cocrystals Correlate with Atomic Polarizability

Thilini P. Rupasinghe, Kristin M. Hutchins, Bimali S. Bandaranayake, Suman Ghorai, Chandana Karunatilake, Dejan-Krešimir Bučar, Dale C. Swenson, Mark A. Arnold, Leonard R. MacGillivray*, and Alexei V. Tivanski*

Department of Chemistry, University of Iowa, Iowa City, IA. 52242-1294, United States

Supporting Information Placeholder

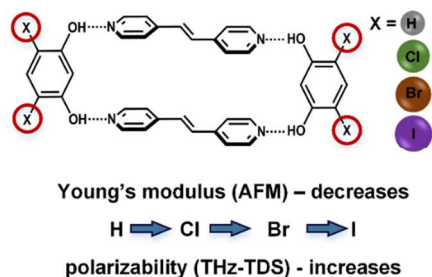
ABSTRACT: A correlation between Young's modulus, as determined by using nanoindentation atomic force microscopy (AFM), and atomic polarizability is observed for members of a series of cocrystals based on systematic changes to one cocrystal component. Time domain spectroscopy over terahertz frequencies (THz-TDS) is used for the first time to directly measure the polarizability of macro- and nano-sized organic solids. Cocrystals of both macro and nano-dimensions with highly-polarizable atoms result in softer solids and correspondingly higher polarizabilities.

Studies on the mechanical properties of organic crystalline solids have gained significant attention owing to potential applications in fields such as pharmaceuticals, electronics, gas storage, biophysics, explosives, and device fabrication.¹⁻⁵ Mechanical property characterization is essential, for example, to achieve materials with increased tabletability in pharmaceuticals and to understand structural changes (*e.g.*, phase transitions).⁶ For device fabrication, especially in flexible electronics, knowledge of mechanical properties is important to establish and optimize operational limits.⁷ Understandings of mechanical properties can also provide insights into relative strengths of intermolecular interactions in solids (*e.g.*, hydrogen bonds), which can serve to link size-dependent structural properties (*e.g.*, elasticity) that span atomic to macroscopic levels.^{8,9,10}

In this context, polarizability is a property of a chemical system that describes the tendency of charge distribution to be distorted in response to an external electric field. At the atomic level, polarizability increases as volume occupied by electrons increases, although much less is known regarding polarizabilities of molecules, assemblies of molecules, and those of corresponding bulk material solids. There is emerging evidence that polarizability can be *inversely* related to the stiffness of a material as measured by its Young's modulus.¹¹⁻¹⁴⁵ Specifically, an inverse relationship between stiffness and atomic or molecular polarizability has been observed for metals, oxides, covalent crystals and polymers.^{9,14-17} A linear relationship between molecular polarizability

and compressibility, which is inversely proportional to Young's modulus, has been also demonstrated in halomethanes.¹¹ A linear relationship has also been noted between Young's modulus and binding energy within graphene nanoribbon materials, which was attributed to the decrease in molecular polarizability.¹² No such relationship has been discussed in the context of organic crystalline solids. Moreover, given that elastic properties of nano-sized materials may differ considerably from larger and extended particles,¹⁸ it will be of paramount importance to determine relationships between polarizability and mechanical properties to facilitate the rational design, or crystal engineering,^{7,8} of novel multi-component solids with controllable and useful physical-chemical properties.

Scheme I. Mechanical properties of cocrystals (res)·(4,4'-bpe) and (4,6-di-X-res)·(4,4'-bpe) (X = Cl, Br, I).



Herein, we present Young's modulus and polarizability measurements on a series of macro- and nano-dimensional organic cocrystals composed of either resorcinol (res) or 4,6-di-X-res (X = Cl, Br, I) and *trans*-1,2-bis(4-pyridyl)ethylene (4,4'-bpe) (Scheme I). From atomic force microscopy (AFM) nanoindentation measurements,¹⁸⁻²³ we show that both macro- and nano-sized cocrystals display a decrease in Young's modulus when the size of the substituent is increased from parent res (H) to Cl to Br to I. A correlation between the Young's modulus and polarizability is demonstrated through both measurements and DFT calculations. Terahertz (THz) time domain spectroscopy (TDS) is also used to directly measure the polarizabilities of

the solids and, in doing so, verify the AFM measurements. Our work, thus, also establishes THz-TDS as a convenient and practical method to gain insight into relationships between atom-to-bulk properties of organic solids.

Our study involves macro- and nano-sized cocrystals of (res)-(4,4'-bpe) **1**, (4,6-di-Cl-res)-(4,4'-bpe) **2**, (4,6-di-Br-res)-(4,4'-bpe) **3** and (4,6-di-I-res)-(4,4'-bpe) **4**. Macro-sized crystals of **1** and **2** were generated as reported.^{24,25} Macro-sized crystals of **3** and **4** were formed *via* slow solvent evaporation of 4,4'-bpe and the appropriate res (1:1 ratio) in EtOH. Formulations of **3** and **4** were confirmed using ¹H NMR spectroscopy and single-crystal X-ray diffraction. Nano-sized cocrystals of **1-4** were readily generated using sonochemistry¹² (See SI).

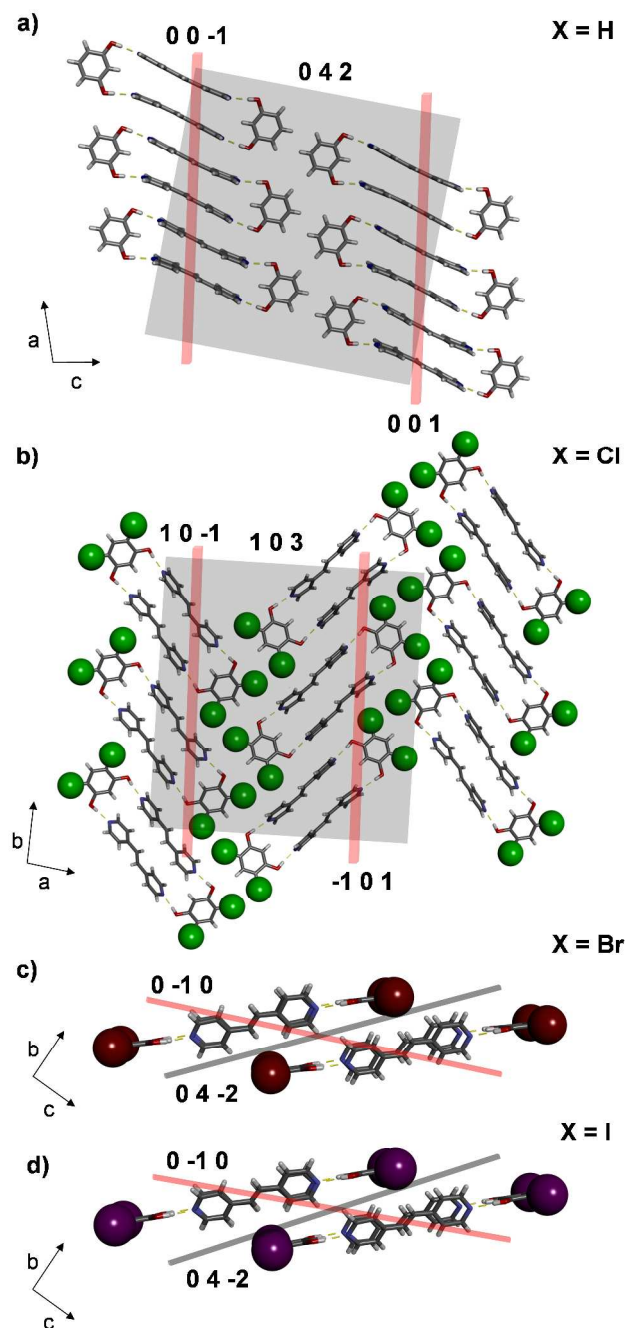


Figure 1. X-ray structures: (a) **1**, (b) **2**, (c) **3**, and (d) **4** highlighting layered packing of assemblies. AFM planes probed for macro-sized crystals highlighted in red. Offset layers highlighted in gray.

Single-crystal X-ray experiments reveal each solid to exhibit a closed hydrogen-bonded tetramer of molecules sustained by four O-H...N hydrogen bonds (O...N separations (Å): O(1)...N(1) 2.71(1), O(2)...N(2) 2.76(1) **3**; O(1)...N(1) 2.77(1), O(2)...N(2) 2.69(1) **4**) (Fig. 1). Cocrystals **1**, **3**, and **4** are isostructural, crystallizing in the triclinic space group $P\bar{1}$, while **2** lies in the monoclinic space group $P2_1/n$.

The tetramers in each cocrystal self-assemble to form offset layers. The tetramers of **1** interact in the crystallographic (042) plane *via* face-to-face π - π forces (C...C: 3.44 Å) of the olefins (Fig. 1a). The layers stack offset along the *b*-axis and interact *via* C-H(pyridine)...O(res) (C...O: 3.33, 3.56 Å) and C-H(pyridine)... π (res) forces (C...C: 3.68 Å). Tetramers of **2** interact in the crystallographic (103) plane *via* Cl...Cl forces (3.55 Å). The Cl...Cl interactions are classified as Type II ($|\theta_1 - \theta_2| = 36^\circ$),²⁶ which define halogen bonds between the res molecules (Fig. 1b). The layers also stack along the *c*-axis *via* C-H(pyridine)... π (res) forces (C...C: 3.63 Å). For **3** and **4**, the tetramers interact in a layer *via* O...Br (3.16 Å, **3**) and O...I (3.22, **4**) forces, respectively (Figs. 1c,d). While the O...Br and O...I distances are shorter than the van der Waals distances, the interactions are Type I ($|\theta_1 - \theta_2| 2^\circ$ (**3**) and 2° (**4**)), which is consistent with strong effects of close packing.²⁶⁻²⁸ The layers stack offset, interacting *via* C-H(pyridine)... π (res) forces (C...C: 3.63 Å **3**, 3.61 Å **4**).

Characterizations of Young's moduli for both macro- and nano-sized samples of **1-4** were carried out using AFM nanoindentation.^{7,18} The macro-sized cocrystals of **1-4** exhibited prism morphologies with bases *ca.* 0.30 × 0.05 mm and heights of *ca.* 0.05 mm. Top and bottom crystal faces that correspond to the crystallographic (001) and (00-1) planes of **1**, (10-1) and (-101) planes of **2**, and (0-10) and (010) planes for **3** and **4** were directly probed by AFM. The planes probed for **1** correspond to the long-axis of a hydrogen-bonded tetramer within a layer, extending along the *c*-axis (Fig. 1a). The planes for **2** are also within a layer, extending along the *a*-axis (Fig. 1b). The planes for **3** and **4** bisect neighboring layers that sit along the *b*-axis (Figs. 1c,d).

Repeated force-displacement curves were recorded on the macro-sized cocrystals at *ca.* 100 positions of both top and bottom faces. Top planes correspond to the initial phase of crystal growth while bottom planes towards the end. Two conclusions are drawn from the histogram data of the Young's moduli measurements (Fig. 2, left column and Table 1).²⁹ First, the top faces for **2-4** show 10-20% higher Young's modulus values relative to the bottom, while the Young's modulus for the top face of **1** is ~20% lower than that for the bottom. The differences may reflect the presence of either hydrogen-bond-donor or -acceptor groups at the individual crystal surfaces (*i.e.* either res or 4,4'-bpe at face).^{18,30} More importantly, the AFM measurements of the cocrystals show a general dependence of the Young's modulus on the nature of the res substituent (Fig. 3a). Specifically, we observe an increase in crystal softness that is correlated with an increase in atomic polarizability¹¹ (H = 0.67, Cl = 2.18, Br = 3.05, I = 4.7 Å³). The relationship is particularly noteworthy for isostructural **1**, **3** and **4**, where the change across the series can be directly attributed to the identity of the H and halogen atoms.

We next studied nano-sized cocrystals (bases ca. $0.8 \times 0.8 \mu\text{m}$ and heights of ca 50-200 nm) where the measurements are expected to yield an orientation averaged response and, thus, are considered more reflective of bulk properties¹⁸ (Fig. 2, Table 1). Specifically, similar to the macro-sized solids, the nano-dimensional cocrystals of **1** exhibited the highest Young's modulus values, followed by **2**, **3**, and **4**. Thus, a systematic decrease in Young's modulus was also observed with increasing atomic polarizability from H to Cl to Br to I (Fig. 3a). The decrease in stiffness was on the order of 55% from H to Cl, 25% from Cl to Br and 42 % from Br to I. The nano-sized X-substituted cocrystals also displayed a size-dependent increase in stiffness compared to the macro-sized solids (33% for **2**, 120% for **3**, 95% for **4**).^{11,18}

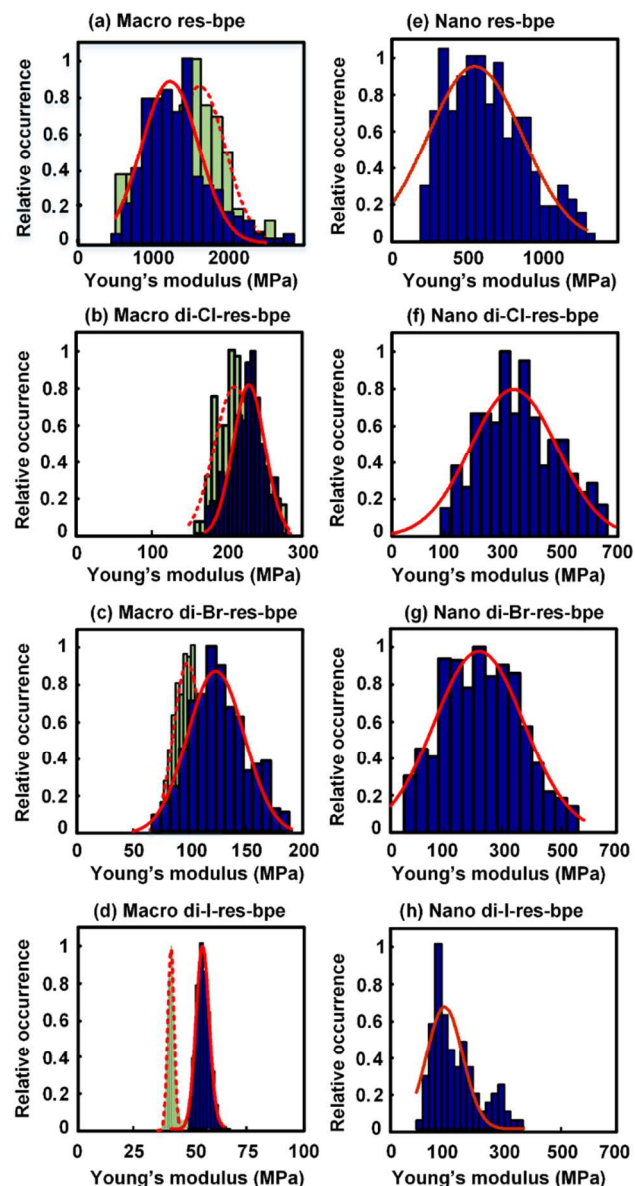


Figure 2. Histograms of Young's modulus for macro- (left) and nano-sized (right) **1-4** (Gaussian fits as red lines). For macro crystals, top plane data in blue bars, bottom plane in green bars.

To probe the observed correlation between Young's modulus and polarizability, we turned to THz-TDS. The coherent nature of THz spectroscopy permits a direct

measure of polarizability as related to dielectric properties. THz-TDS is a rapidly-developing technique that uses electromagnetic radiation (0.3 to 4.0 THz) to provide information related to vibrations in crystalline solids, intermolecular interactions in liquids, and rotational transitions in gases.³¹⁻³³ Dielectric constants were, thus, determined for **1-4** from 10 to 20 cm^{-1} . The constants were determined within 4-5 min by measuring the delay in a THz pulse transmitted across a pressed pellet composed of 5% cocrystal embedded within a matrix of polytetrafluoroethylene. Average values from measurements over several pellet preparations were used to calculate polarizability using the Clausius-Mossotti relationship (see SI).³⁴⁻³⁵ Given the nature of the dielectric measurements, the resulting polarizability values correspond to ensemble measurements over a population of crystals randomly oriented with respect to the optical axis of the THz pulse, thereby, representing an average property of **1-4**.

Table 1: Young's modulus (YM) and polarizability (α) measurements (crystallographic plane in

SAMPLE	YM (MPa)	α (\AA^3)
1-macro	1600 ± 350 (00-1)	88.5 ± 1.6
	1250 ± 350 (001)	
2-macro	270 ± 25 (10-1)	93.1 ± 0.7
	235 ± 25 (-101)	
3-macro	120 ± 15 (0-10)	98.3 ± 0.6
	95 ± 10 (010)	
4-macro	54 ± 3 (0-10)	104.1 ± 1.4
	40 ± 2 (010)	
1-nano	570 ± 200	87.6 ± 1.4
2-nano	370 ± 140	89.6 ± 1.0
3-nano	275 ± 140	97.5 ± 1.7
4-nano	160 ± 50	102.2 ± 1.3

parentheses).

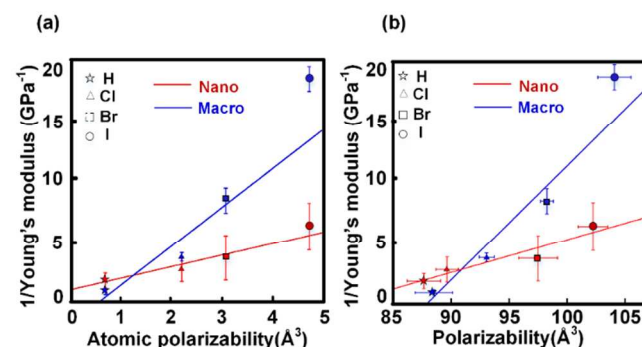


Figure 3. Plots: (a) inverse Young's modulus vs atomic polarizability for **1-4** (weighted fit macro $R^2=0.85$, nano $R^2=0.93$) and (b) inverse Young's modulus vs polarizability from THz-TDS for **1-4** (weighted fit macro $R^2=0.93$, nano $R^2=0.93$). Data for macro-sized crystals for top plane (see SI for plot using bottom plane data).

In general, the measured polarizability values were comparable to benzoic acid, sucrose, and thymine as

determined from THz-TDS measurements on single crystals (Fig. 3 and Table 1).³⁶ Moreover, the polarizabilities from the THz-TDS measurements display a clear correlation (weighted fit macro $R^2=0.93$, nano $R^2=0.93$) with inverse Young's modulus obtained using AFM measurements (95% confidence limit) (Fig. 3b). These results also agree qualitatively with DFT calculations using the RB3LYP method (see SI).^{37,38} Hence, the polarizabilities of the solids increase with increasing size of the res substituent, which corresponds to the decrease in stiffness consistent with the expected inverse relationship.

While the correlation between Young's modulus and atomic polarizability in 1-4 may seem surprising given the highly-anisotropic nature of organic crystals, two features of the crystal structures of 1-4 are noteworthy in relation to the mechanical data. First, the tetramers in each cocrystal assemble to form layers. That the components maintain layers across the series is likely a consequence of the isosteric relationship between the res derivatives. Atoms with comparable volumes are considered isosteric, while molecules that differ only in substitution of isosteres at a specific position are generally expected to form similar crystal structures.³⁹ Even the anomalous behavior of 2 in forming Type II halogen bonds^{26,40} is unable to circumvent a tendency of the hydrogen-bonded tetramers to form a layered structure. The structural similarities of 1-4, thus, allow the data from the AFM measurements to be directly compared between the solids. Second, the interactions between the tetramers involve numerous weak and dispersive forces,⁴¹ with the interactions involving the halogen atoms in 2-4 being considerably weak. Indeed, the O...X interactions in 3 and 4, which are generally considered stronger than those of Cl...Cl forces in 2,²⁷ fall within the definition of a weaker Type I halogen interaction wherein organization in the solid state arises owing to strong contributions of close packing.²⁶ Thus, in the absence of any particularly strong inter-tetramer forces⁴¹ yet with layers pervading across the series, the general increase in softness and polarizability from 1 (H) to 4 (I) can be ascribed to the differences in atomic composition of the res components.

In this report, we have demonstrated that a bulk mechanical property in the form of Young's modulus for a series of organic cocrystals is correlated to atomic polarizability. The inverse relationship has been verified using THz-TDS, which establishes the analytical technique as a rapid and convenient method to obtain polarizability data related to atomic, molecular, and supramolecular structure. Given the now demonstrated relationship between chemical structure and physical properties, we expect present and future findings to establish atomic-to-bulk correlations that enable the rational design of a variety of multicomponent materials with desired mechanical and chemical properties.

ASSOCIATED CONTENT

Supporting Information

Experimental details, AFM height images of macro- and nano-sized cocrystals, nanoindentation analysis, single crystal and powder X-ray diffraction data, Terahertz spectra and theoretical calculations. This material is available free of charge via the Internet at <http://pubs.acs.org>. Supplementary crystallographic data (CCDC 1025228, 1025229) can be

obtained free of charge from the Cambridge Crystallographic Data Centre via www.ccdc.cam.ac.uk/conts/retrieving.html.

AUTHOR INFORMATION

Corresponding Author

alexei-tivanski@uiowa.edu
len-macgillivray@uiowa.edu

ACKNOWLEDGMENT

T.P.R. and A.V.T. gratefully acknowledge financial support from the National Oceanic and Atmospheric Administration (NOAA) Climate Program Office, Earth System Science Program, award NA11OAR4310187. L.R.M. gratefully acknowledges partial financial support from the National Science Foundation (DMR-1408834).

REFERENCES

- (1) Kosa, M.; Tan, J. C.; Merrill, C. A.; Krack, M.; Cheetham, A. K.; Parrinello, M. *ChemPhysChem* **2010**, *11*, 2332.
- (2) Kim, T.; Zhu, L. Y.; Al-Kaysi, R. O.; Bardeen, C. J. *ChemPhysChem* **2014**, *15*, 400.
- (3) Vogelsberg, C. S.; Garcia-Garibay, M. A. *Chem. Soc. Rev.* **2012**, *41*, 1892.
- (4) Nath, N. K.; Panda, M. K.; Sahoo, S. C.; Naumov, P. *CrystEngComm* **2014**, *16*, 1850.
- (5) Bolton, O.; Matzger, A. J. *Angew. Chem. Int. Ed.* **2011**, *50*, 8960.
- (6) Mishra, M. K.; Varughese, S.; Ramamurty, U.; Desiraju, G. R. *J. Am. Chem. Soc.* **2013**, *135*, 8121.
- (7) Reddy, C. M.; Krishna, G. R.; Ghosh, S. *CrystEngComm* **2010**, *12*, 2296.
- (8) Varughese, S.; Kiran, M. S. R. N.; Ramamurty, U.; Desiraju, G. R. *Angew. Chem. Int. Ed.* **2013**, *52*, 2701.
- (9) Hooks, D. E.; Ramos, K. J.; Bolme, C. A.; Cawkwell, M. J. *Propellants, Explosives, Pyrotechnics* **2015**, *40*, 333.
- (10) Ramos, K. J.; Bahr, D. F. *Journal of Materials Research* **2007**, *22*, 2037.
- (11) Donald, K. J. *J. Phys. Chem. A* **2006**, *110*, 2283.
- (12) Zeinalipour-Yazdi, C. D.; Christofides, C. J. *Appl. Phys.* **2009**, *106*, 054318-1.
- (13) Gilman, J. J. *Mater. Res. Innovations* **1997**, *1*, 71.
- (14) Gilman, J. J. *Electronic basis of the strength of materials*; 1st ed.; Cambridge University Press: New York, 2003.
- (15) Gilman, J. J. *Chemistry and Physics of mechanical hardness*; 3rd ed ed.; Wiley: New Jersey, 2009.
- (16) Noorzadeh, S.; Parhizgar, M. *Journal of Molecular Structure: THEOCHEM* **2005**, *725*, 23.
- (17) Gilman, J. J. *AIP Conference Proceedings* **2006**, *845*, 855.
- (18) Karunatilaka, C.; Bučar, D.-K.; Ditzler, L. R.; Friščić, T.; Swenson, D. C.; MacGillivray, L. R.; Tivanski, A. V. *Angew. Chem. Int. Ed.* **2011**, *50*, 8642.
- (19) Ramamurty, U.; Jang, J. I. *CrystEngComm* **2014**, *16*, 12.
- (20) Cook, R. F. *Science* **2010**, *328*, 183.
- (21) Shulha, H.; Zhai, X. W.; Tsukruk, V. V. *Macromolecules* **2003**, *36*, 2825.
- (22) Guo, S.; Akhremichev, B. B. *Langmuir* **2008**, *24*, 880.
- (23) Tranchida, D.; Kiflie, Z.; Acierno, S.; Piccarolo, S. *Meas. Sci. Technol.* **2009**, *20*.
- (24) MacGillivray, L. R.; Reid, J. L.; Ripmeester, J. A. *J. Am. Chem. Soc.* **2000**, *122*, 7817.
- (25) Sokolov, A. N.; Bučar, D.-K.; Baltrusaitis, J.; Gu, S. X.; MacGillivray, L. R. *Angew. Chem. Int. Ed.* **2010**, *49*, 4273.
- (26) Mukherjee, A.; Tothadi, S.; Desiraju, G. R. *Acc. Chem. Res.* **2014**, *47*, 2514.
- (27) Cao, D.; Hong, M.; Blackburn, A. K.; Liu, Z. C.; Holcroft, J. M.; Stoddart, J. F. *Chem. Sci.* **2014**, *5*, 4242.
- (28) Mukherjee, A.; Desiraju, G. R. *IUCr* **2014**, *1*, 49.

1 (29) The determined values are comparable to similar cocrystals
2 of (5-CN-res):(4,4'-bpe) (260 MPa), protein crystals (165 MPa), and
3 hyperbranched macromolecules (190 MPa).

4 (30) Bracco, G.; Acker, J.; Ward, M. D.; Scoles, G. *Langmuir* **2002**,
5 *18*, 5551.

6 (31) Smith, R. M.; Arnold, M. A. *Appl. Spectrosc. Rev.* **2011**, *46*, 636.

7 (32) Zeitler, J. A.; Taday, P. F.; Pepper, M.; Rades, T. J. *Pharm. Sci.*
8 **2007**, *96*, 2703.

9 (33) Nguyen, K. L.; Friščić, T.; Day, G. M.; Gladden, L. F.; Jones, W.
10 *Nat. Mater.* **2007**, *6*, 206.

11 (34) Looyenga, H. *Physica* **1965**, *31*, 401.

12 (35) Naftaly, M.; Miles, R. E. *J. Appl. Phys.* **2007**, *102*.

13 (36) Jepsen, P. U.; Clark, S. J. *Chem. Phys. Lett.* **2007**, *442*, 275.

(37) Castro, R.; Berardi, M. J.; Cordova, E.; deOlza, M. O.; Kaifer,
A. E.; Evanseck, J. D. *J. Am. Chem. Soc.* **1996**, *118*, 10257.

(38) Hinchliffe, A.; Perez, J. J.; Machado, H. J. S. *Electron. J. Theor.*
Ch. **1997**, *2*, 325.

(39) Dikundwar, A. G.; Pete, U. D.; Zade, C. M.; Bendre, R. S.;
Row, T. N. G. *Cryst. Growth Des.* **2012**, *12*, 4530.

(40) Type II interactions are less favored for Cl and we note that
these interactions are relatively weak. The $|\theta_1-\theta_2|$ lies just above the
30° threshold.

(41) Ghosh, S.; Mishra, M. K.; Kadambi, S. B.; Ramamurty, U.;
Desiraju, G. R. *Angew. Chem. Int. Ed.* **2015**, *54*, 2674.

Table of Contents

